# Synthesis and studying of structural, surface topography and optical properties of MgxZn1-xO thin Films by spray pyrolysis method

**Mustafa D. Jaafer**

Directorate of Education in Al Najaf, Ministry of Education, Iraq

**Abstract:**

In the present paper, $Mg_xZn_{1-x}O$ thin films were synthesized with a wide composition range x=(0.25, 0.5, 0.75) using a spray polyposis technique at 450 °C. The X-ray data analysis revealed that the films were polycrystalline with hexagonal and cubic structures. The preferential orientation of all films was absorbed along (002). Structural parameter such as average crystallite size, dislocation density and micro-striation were also investigated. AFM results show that the surface topography and the surface quality of the deposited thin film can be controlled by the $Mg^{2+}$ content of $Mg_xZn_{1-x}O$ thin films. The UV-Visible analysis show that the optical absorption values decrease with the increase of $Mg^{2+}$ concentration. It is observed that the band gap increases as the $Mg^{2+}$ concentration increases. The reflectance spectra of $Mg_xZn_{1-x}O$ thin films shifted towards the lower wavelength with the increase of $Mg^{2+}$ concentration. The extinction coefficient was slightly decreased and shifted towards higher energies with the increase of $Mg^{2+}$ contents. These results demonstrate the high quality of single crystal $Mg_xZn_{1-x}O$ films and their potential in high-performance deep ultraviolet optoelectronic devices.

**Keywords:** Spray Pyrolysis method; $Mg_xZn_{1-x}O$ thin films; Structure and Optical properties.

## تحضير ودراسة الخصائص التركيبية وطبوغرافية السطح والبصرية لأغشية $Mg_xZn_{1-x}O$ الرقيقة بالرش الحراري

**مصطفى ضياء جعفر**

مديرية التربية في محافظة النجف , وزارة التربية , العراق

**الخلاصة:**

في هذا البحث، تم تحضير اغشية رقيقة $Mg_xZn_{1-x}O$ مع تراكيز متغيرة x=(0.25, 0.5, 0.75) باستخدام تقنية الرش الحراري عند درجة $450\ ^0C$. اظهرت نتائج فحص حيود الأشعة السينية أن الاغشية كانت متعددة التبلور بتراكيب سداسية ومكعبة. ووجد ان الاتجاه المفضل جميع الاغشية على طول المستوي (002). كما تم قياس المعلمات التركيبية مثل متوسط حجم البلورات، وكثافة تمركز البلورات، والمسافة بين البلورات. وأظهرت نتائج AFM أن تضاريس السطح وجودة السطح من الاغشية الرقيقة يمكن السيطرة على $Mg^{2+}$ من قبل تراكيز اغشية $Mg_xZn_{1-x}O$. وأظهر تحليل الفحوصات البصرية للأشعة المرئية - فوق البنفسجية أن قيم الامتصاص البصري تنخفض مع زيادة تركيز $Mg^{2+}$. ويلاحظ أن فجوة الطاقة تزداد مع زيادة تركيز $Mg^{2+}$. ان طيف الانعكاسية لأغشية $Mg_xZn_{1-x}O$ أزيح نحو الطول الموجي الاقل مع زيادة تركيز $Mg^{2+}$. كذلك انخفض معامل الخمود قليلا وأزيح نحو طاقات أعلى مع زيادة تركيز $Mg^{2+}$. هذه النتائج تثبت جودة عالية لأغشية $Mg_xZn_{1-x}O$ احادية التبلور , ايضاً امكانية عالية الأداء للنبائط الكهروضوئية فوق البنفسجية .

**الكلمات المفتاحية:** طريقة الرش الحراري, اغشية $Mg_xZn_{1-x}O$ الرقيقة , الخصائص التركيبية والبصرية.

## 1. Introduction

ZnO based alloys (including MgZnO, CdZnO, and MnZnO) have been becoming a more and more effective (field of research nowadays )[1]

A decisive step in designing new optoelectronic devices is the realization of band-gap engineering to quantum wells in device heterostructures and create barrier layers. In order to achieve such optoelectronic devices, two significant requirements should be satisfied, one is modulation of the band gap and the other is p-type doping of ZnO. While p type doping of ZnO is beneath intensive research, the latter has been demonstrated by the expansion of $Mg_xZn_{1-x}O$ and $Cd_xZn_{1-x}O$ alloys, allowing modification of band gap in a wide range [2,3,4].

$Mg_xZn_{1-x}O$ is an ideal material for UV detecting because it possesses high visible transparency, high UV absorption coefficients [5,6] and big tunable band gap energy range (3.37–7.8 eV) [7,8].

$Mg_xZn_{1-x}O$ has two crystal structures, cubic (rocksalt) and hexagonal (wurtzite) structure. According to the phase diagram the maximum integration of ZnO in hexagonal structure of MgO is 4%, which is much bigger than 56% of MgO in cubic structure ZnO . In $Mg_xZn_{1-x}O$ the band gap is shifted to higher energies and $Cd_xZn_{1-x}O$ to lower energies compared to ZnO [4,5]. Within the latter few years, different physical deposition techniques have been used for the deposition of $Cd_xZn_{1-x}O$ thin films such as RF reactive magnetron sputtering [9,10], thermal evaporation [11], plasma-assisted molecular beam epitaxy and pulsed laser deposition [12, 13]. Moreover, as a semiconductor material, $Mg_xZn_{1-x}O$ has lately attracted important attention because many improvements in deposition techniques made it possible to develop high quality $Mg_xZn_{1-x}O$ thin films. Spray Pyrolysis deposition (CSP) is a simple technique in which no high quality substrates are wanted; as well as a non-vacuum system. The technique is more appropriate for large area coatings. Therefore, present research work presents in this paper shows the effect of the three different types of substrate regarding their structural, morphological and optical properties of $Mg_xZn_{1-x}O$ films grown by CSP method.

## 2. Experiment

$Mg_xZn_{1-x}O$ thin films have been deposited onto the glass substrates at 450 $^oC$. With different $Mg^{2+}$ concentrations (for x= 0.25, 0.5 and 0.75) using chemical spray pyrolysis method. Here x represents the concentration in the spraying solution. Glass substrates cleaning by distilled water and remove powder and they were placed in double distilled water for 10 min each in an ultrasonic bath, the beaker containing alcohol with high purity (15 min) to remove any dust. So as to prepare $Mg_xZn_{1-x}O$ thin films, magnesium sulfate ($MgSO_4$) and Zinc Sulfate Heptahydrate ($ZnSO_4.7H_2O$) were used as $Mg^{2+}$ and $Zn^{2+}$ ions respectively. The stock solutions of ($MgSo_4$) and ($ZnSO_4.7H_2O$) (0.1M) were prepared. To take homogeneity of uniform deposition each solution was stirred for 10 minute before the film deposition. The starting solution was mixed thoroughly and latter solution was sprayed. Through the spraying process, the substrates were heated by electrically heating the copper plate. The optimized coating parameters used in the present act as substrate-nozzle distance-30 cm flow rate of the precursor solution-8 ml/min utilized as a carrier gas. Substrate temperature was controlled by means of Iron-Constantan thermocouple. To investigate the effects of $Mg^{2+}$ concentration on the films, three series of samples (0.25, 0.5, 0.75 M%) were produced. The structural properties of all the films were studied by XRD-6000 Shimadzuautomatic diffractometer using Cu:Kα radiations (λKα=1.5406 Å). The optical absorption and transmittance spectra were recorded from (300-800) nm wavelength using Shimadzu UV-1650 Pc UV-VIS scanning spectrophotometer at room temperature.

## 3. Result and Discussion:

Fig.1 shows the XRD spectra of $Mg_xZn_{1-x}O$ thin films prepared for different $Mg^{2+}$ concentrations deposited at 450°C. All the peaks of the ZnO thin films correspond with the peaks of standard ZnO (JCPDS Card No. 36-1451). Most of the peaks assigned to, (002), (101), (102), (110), (103) and (202) polycrystalline phase and orientations of hexagonal (wurtzite) phase of ZnO. As well as, (200), (311) and (222) peaks of MgO cubic (rocksalt) polycrystalline phases of standard (JCPDS Card No. 43-1022).

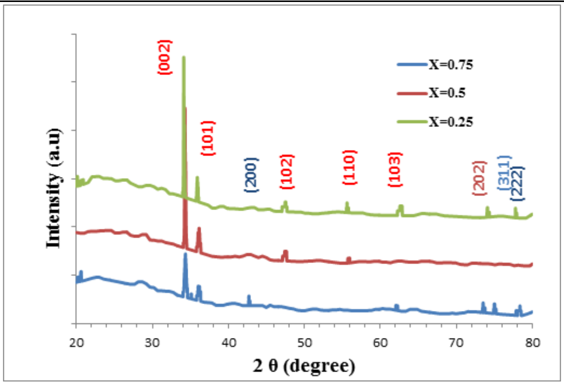


**Fig.1:** Shows the x-ray diffraction pattern of $Mg_xZn_{1-x}O$ thin films, a function of Mg composition X=(0.25, 0.5, 0.75)

The spectra indicated hexagonal (wurtzite) crystal structure for the thin films that retained the preferential (002) peak growth along the c-axis of the films. The intensity of (002) peak is relatively higher than that of the intensity of other peaks such as (101) for all the $Mg^{2+}$ concentrations used in this work. However, the intensity of (002) and (101) peaks decreases and shifts towards high 2θ angles as the $Mg^{2+}$ content increases. This outcome suggests that the lattice parameter along the c-axis decreases indicating a compressive strain [14]. This result is harmonic with almost all previous studies [15].

The lattice constant *a* and *c* for hexagonal planes of $Mg_xZn_{1-x}O$ thin films are calculated from XRD data using the following equation[16].

$$\frac{1}{d^2}=\frac{4}{3}\left(\frac{h^2+hk+k^2}{a^2}\right)+\frac{\ell^2}{c^2}.------(1)$$

They $(hkl)$ are Miller indices, The a parameter is obtained from the plane $(h00)$, while the plane $(00l)$ is used to obtain c-parameter. Table 1. the x-ray data analysis data of $Mg_xZn_{1-x}O$ thin films. It had been reported that the $Mg^{2+}$ incorporation into ZnO lattice usually cause the decrease of the c-axis length, because the ionic radius of $Mg^{2+}$ (0.57 A°) was slightly smaller than that of $Zn^{2+}$ (0.60 A°). The crystallite size (D) was calculated from XRD data using Debye Scherrer formula below[17].

$$G.Z=0.9\lambda/B\cos\theta------(2)$$

*λ:* is the wavelength, B: the full width half maximum (FWHM), *Θ*: is Bragg diffraction angle. The crystallite size of the $Mg_xZn_{1-x}O$ increased with decreased in $Mg^{2+}$ composition from106 nm to 69.22 nm with increase shown in fig.2. and Table

1. This behavior is observed in previous works [18].

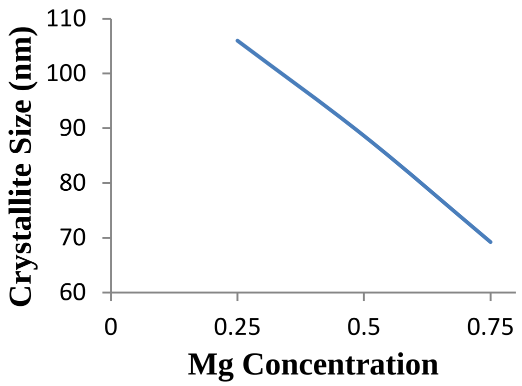


**Fig. 2:** Variation of crystallite size of $Mg_xZn_{1-x}O$ thin films, a function of $Mg^{2+}$ concentration for (002) plane.

The dislocation density (δ) of $Mg_xZn_{1-x}O$ thin films is defined as the number of dislocation lines per unit volume and determined from the relation [25, 26]:

$$\delta = \frac{n}{D^2} \qquad ---------(3)$$

Where n=1, it always indicate the minimum dislocation density of thin film and D is the crystallite size. The number of crystallites per unit surface area (N) could be calculated according to [25, 26]:

$$\boldsymbol{N} = \frac{\boldsymbol{t}}{(\boldsymbol{D})^3} \qquad (\boldsymbol{4})$$

the t is the thickness of the film. Fig. 3. shows δ and N as a function of $Mg^{2+}$ concentration, it is absorbed that N has the same behavior of δ were they increasing with the increasing of $Mg^{2+}$ concentration. The small value of (δ) obtained in the present paper confirms that the spray pyrolysis is an effective technique can be used to deposit good and high-quality $Mg^{2+}$ concentration for $Mg_xZn_{1-x}O$ thin film [14].

The values of calculated δ and N with respect to the $Mg^{2+}$ concentration shown in table 1. The micro-strain ($\varepsilon$) has been determind using the following equation [25, 26], and then the values are presented in table 1.

$$\text{Micro-Strain } (\varepsilon) = \frac{B \cos\theta}{4} \quad -----------(5)$$

Fig. 4. shows the ($\varepsilon$) in the films for (002) peak is initially decreased with increasing $Mg^{2+}$ concentrations from (8.511 to 4.794). The type of micro-strain change can be attributed to the ionic radius of $Zn^{2+}$ ions which is slightly higher than $Mg^{2+}$ ions, the strain in ZnO lattice is influenced by $Mg^{2+}$ and thereby alters the preferential growth. Thus the results show that Mg content reduces the micro-strain of the $Mg_xZn_{1-x}O$ thin films.

Table 1: The x-ray data analysis data of $Mg_xZn_{1-x}O$ thin films a function of $Mg^{2+}$ composition X=(0.25, 0.5, 0.75)

| Mg Concretion | (hkl) | 2Θ | FWHM deg | d(A°) Observed | a (A°) | C (A°) | Crystallite Size (nm) | Dislocation Density (δ) $10^5$ Lines/m$^2$ | (N) $10^{16}$ m$^{-2}$ | Micro Strain (e) $10^3$ |
|---|---|---|---|---|---|---|---|---|---|---|
| 0.25 | 002 | 34.32 | 0.2362 | 2.6127 | 2.87 | 4.72 | 106 | 0.889 | 1.25 | 8.511 |
| | 101 | 36.09 | 0.3149 | 2.4884 | | | | | | |
| | 200 | 42.70 | 0.0590 | 2.1175 | | | | | | |

| | | | | | | | | | | |
|---|---|---|---|---|---|---|---|---|---|---|
| | 103 | 62.08 | 0.0720 | 1.4937 | | | | | | |
| | 202 | 73.52 | 0.0840 | 1.2870 | | | | | | |
| | 311 | 75.07 | 0.6298 | 1.2652 | | | | | | |
| | 222 | 78.21 | 0.2880 | 1.2211 | | | | | | |
| 0.5 | 002 | 34.28 | 0.0840 | 2.6131 | 3.01 | 5.22 | 88.62 | 1.273 | 2.15 | 3.028 |
| | 101 | 36.09 | 0.0840 | 2.6118 | | | | | | |
| | 102 | 47.41 | 0.4800 | 1.9158 | | | | | | |
| | 110 | 55.92 | 0.4690 | 1.6465 | | | | | | |
| 0.75 | 002 | 34.13 | 0.0590 | 2.6266 | 3.03 | 5.25 | 69.22 | 2.08 | 4.52 | 4.794 |
| | 101 | 35.90 | 0.1181 | 2.5013 | | | | | | |
| | 102 | 47.39 | 0.6298 | 1.9182 | | | | | | |
| | 110 | 55.61 | 0.1181 | 1.6525 | | | | | | |
| | 103 | 62.76 | 0.4723 | 1.4847 | | | | | | |
| | 202 | 74.09 | 0.0840 | 1.2785 | | | | | | |
| | 222 | 77.73 | 0.0840 | 1.2328 | | | | | | |

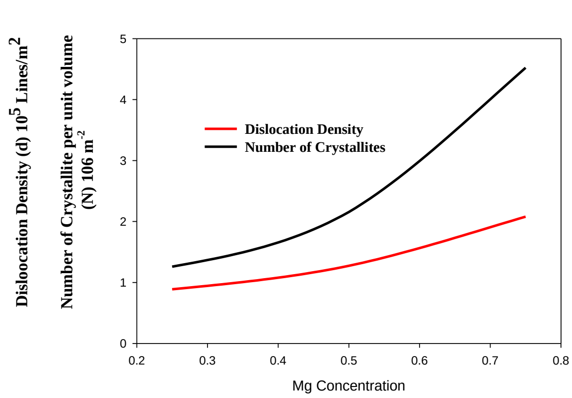


**Fig. 3:** The variation (δ) and (N) of $Mg_xZn_{1-x}O$ thin films, a function of $Mg^{2+}$ concentration for (002) plane

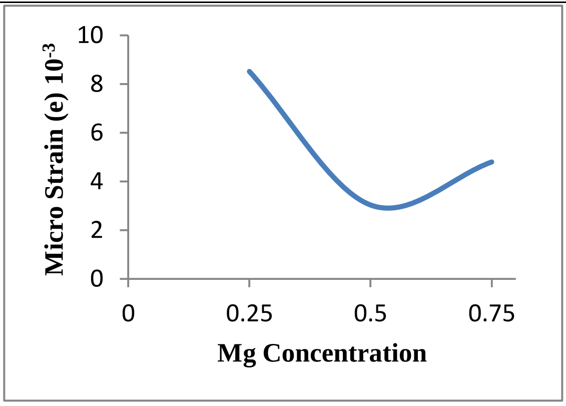


**Fig.4:** The variation of The micro-strain ($\varepsilon$) of $Mg_xZn_{1-x}O$ thin films a function of $Mg^{2+}$ concentration for (002) plane.

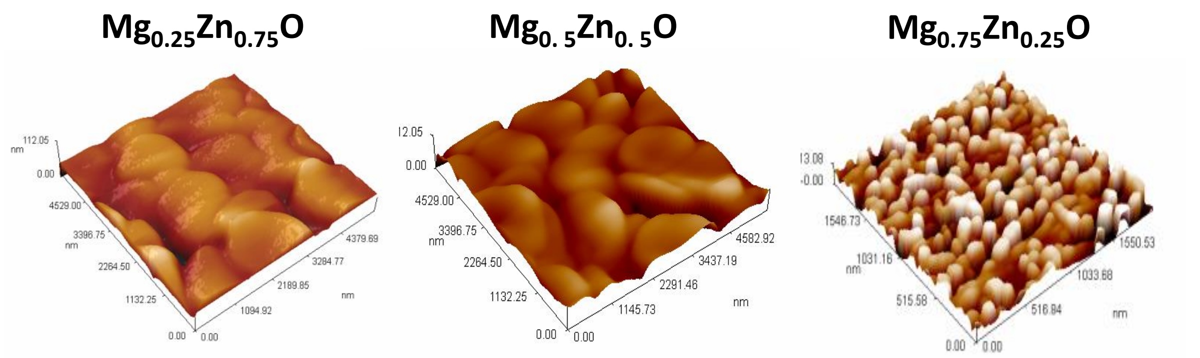


**Fig. 5:** Shows the AFM images diffraction pattern of $Mg_xZn_{1-x}O$ thin films, a function of $Mg^{2+}$ composition X=(0.25, 0.5, 0.75)

Fig. 5. shows AFM images of $Mg_xZn_{1-x}O$ thin film. It observed smooth and uniform surface of $Mg^{2+}$ composition X=(0.25, 0.5), while the $Mg^{2+}$ composition X=(0.75) has grainy patterns. With increasing $Mg^{2+}$ content, the surface RMS roughness increases from 3.23 nm, 8.87 nm to 9.04 nm as x varied from 0.25, 0.5

and 0.75 respectively shown in the table 2. The increase in the RMS roughness is attributed to the partial padding of $Mg^{2+}$ in the pores. From the( results above), it is seen clearly that an improvement of the microstructure and the crystalline quality of the $Mg_xZn_{1-x}O$ composite as the $Mg^{2+}$ content increased. This result is in good agreement with [23]. The grain size is increased from 100 to 148 nm for $Mg^{2+}$ composition X=(0.25, 0.5) while for $Mg^{2+}$ composition X=(0.75) they are a reduced to 101 nm. Results of grain size for AFM images are roughly consistent with crystallite size results for X-Ray analysis. These results demonstrate the high quality polycrystalline $Mg_xZn_{1-x}O$ films and their potential in high-performance deep ultraviolet optoelectronic devices.[19].

**Table 2: The optical band gab, RMS and grain size for AFM image of $Mg_xZn_{1-x}O$ thin films**

| Number | Material | Band gap (eV) | Wavelength (nm) | Roughness Average nm | Root mean square nm | Grain size nm |
|---|---|---|---|---|---|---|
| 1 | $Mg_{0.75}Zn_{0.25}O$ | 4.01 | 498.9 | 9.04 | 12.1 | 101 |
| 2 | $Mg_{0.5}Zn_{0.5}O$ | 3.88 | 464.5 | 8.87 | 12.3 | 148 |
| 3 | $Mg_{0.25}Zn_{0.75}O$ | 3.28 | 462.5 | 3.23 | 3.73 | 100 |

Fig. 6. shows the absorption spectra of the deposited $Mg_xZn_{1-x}O$ thin films with (0.25, 0.5 and 0.75) $Mg^{2+}$concentrations, respectively. The fig.3 reveals that with decreasing enrichment of $Mg^{2+}$ concentration the band edge shift to lower wavelength (blue shift). As grown x=0.25 has a band edge at~345 nm. It monotonously blues shifted with increasing $Mg^{2+}$ concentration, finally reaching a value of ~310 nm at x=0.75.

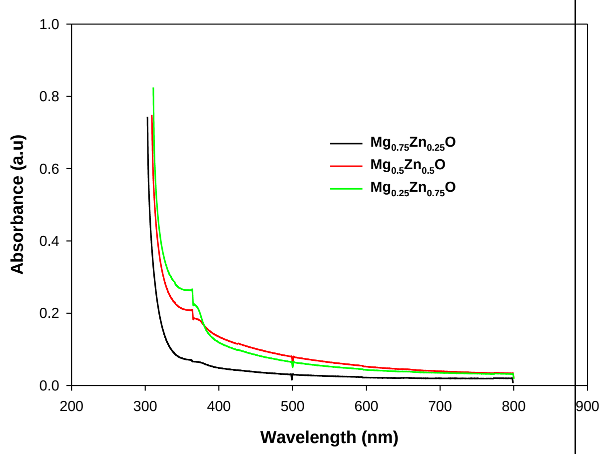


**Fig. 6:** Shows the Absorption spectra of $Mg_xZn_{1-x}O$ thin films, a function of Mg composition X=(0.25, 0.5, 0.75).

The optical transmittance spectra of the $Mg_xZn_{1-x}O$ thin films with different x values were obtained, and steep absorption edges were observed demonstrating that the thin films are homogeneous.

The difference of transmittance against wavelength for different composition x is presented in Fig. 7. It was observed that transmittance is increased with the increase of the $Mg^{2+}$ content in the $Mg_xZn_{1-x}O$ thin films. The transmittance varies from 70% to 40% as x varies from 0.75 to 0.25 in the 350–800 nm due to evidencing the substitution incorporation of $Mg^{2+}$ into the $Zn^{2+}$ site of the wurtzite lattice.

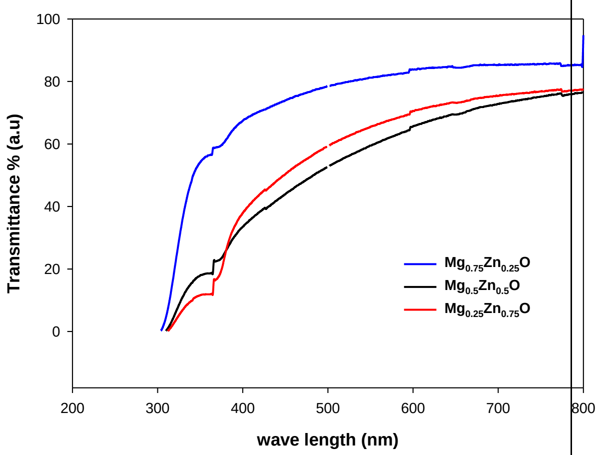


**Fig. 7:** Shows the Transmittance spectra of $Mg_xZn_{1-x}O$ thin films, a function of Mg composition X=(0.25, 0.5, 0.75)

The energy gap values depend in general on the film crystal structure, the arrangement and distribution of atoms in the crystal lattice, also it is affected by crystal regularity.

The band gap energy $E_g$ was calculated by using relationship [20]:

$$\alpha h\upsilon = B\,(h\,\upsilon - E_g\,)^{\,r} \qquad \text{--------(3)}$$

*B*, *α*, *hν* are constant, absorption coefficient and energy photon respectively. The optical band gap ($E_g$) of the thin film to be determined by the experimentally observed values of $(\alpha h\nu)^2$ against (hν) are plotted in Fig. 8. The band gaps (Eg) of the $Mg_xZn_{1-x}O$ thin films were tuned from 3.82 eV to 4.01 eV by tuning the incorporation of $Mg^{2+}$ ion concentration in the CSP. In other words, the optical energy band gap of $Mg_xZn_{1-x}O$ thin films become wider as $Mg^{2+}$ content increases. This increase can be imputed to the Burstein-Moss effect and/or to the forming of hexagonal $Mg_xZn_{1-x}O$ alloy phase [7, 22].

The study revealed that the fabricated films can use as ultraviolet (UV) photodetectors in many optoelectronic devices such as missile warning and tracking, chemical/biological agent detecting, and engine/flame monitoring [21]. The optical band gap with the crystallite size and $Mg^{2+}$ content of $Mg_xZn_{1-x}O$ film are illustrated in fig. 9. It is observed that the energy band gap decreases with increasing crystallite size while it increased with increased $Mg^{2+}$ content.

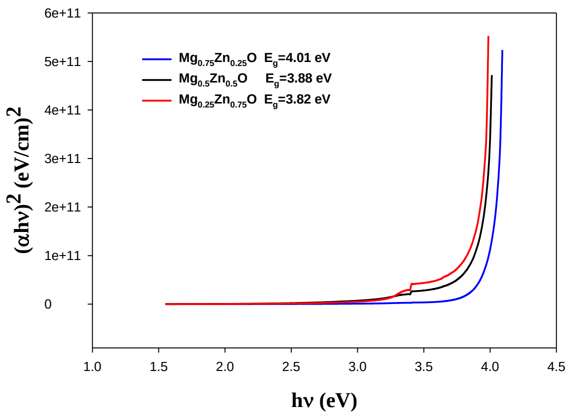


**Fig.8:** Optical band gap (Eg) of $Mg_xZn_{1-x}O$ thin films, a function of $Mg^{2+}$ composition X=(0.25, 0.5, 0.75).

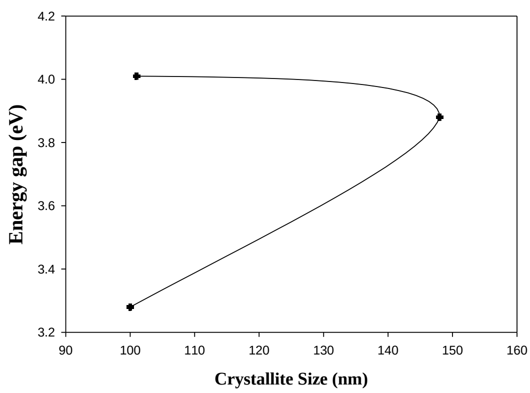

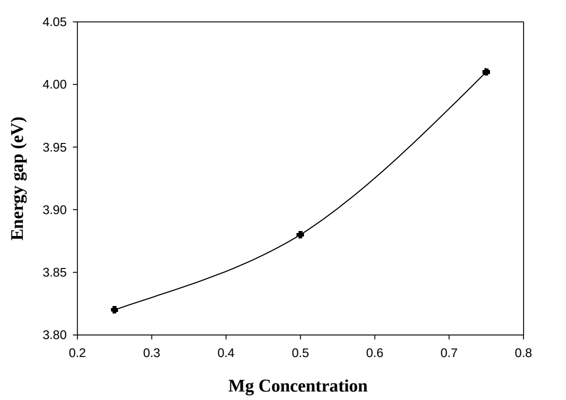


**Fig. 9:** The variation of the optical energy gap with crystallite size and with $Mg^{2+}$ concentration.

The reflective (*R*) $Mg_xZn_{1-x}O$ thin films was calculated by using Eq. [19] below.

$$R+T+A=1 \quad \text{--------------------(4)}$$

where, *T* is transmittance , *A* is absorption.

Fig.10. depicts the reflectance spectra at room temperature for $Mg_xZn_{1-x}O$ thin films. The reflectance shifted towards the lower wavelength (high energies) with increasing $Mg^{2+}$ content due to the effect of surface morphology on the $Mg_xZn_{1-x}O$ thin films.

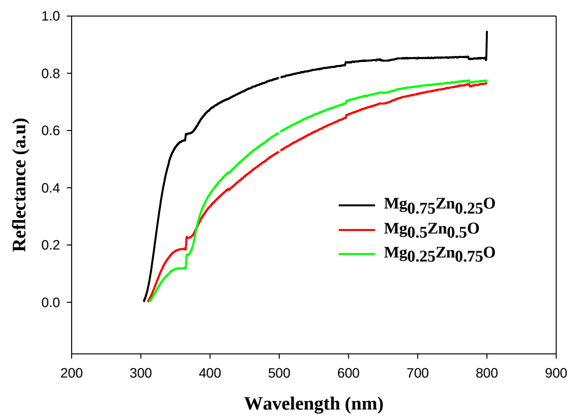


**Fig. 10:** Shows the Reflective (R) of $Mg_xZn_{1-x}O$ thin films, a function of $Mg^{2+}$ composition X=(0.25, 0.5, 0.75)

Fig.11. shows the extinction coefficient for $Mg_xZn_{1-x}O$ films grown at various $Mg^{2+}$ concentrations (x=0.25, 0.5 and 0.75) as a function of photon energy. The extinction coefficient (*k*) of $Mg_xZn_{1-x}O$ thin films was calculated using Eq. [20] below.

$$K = \frac{\alpha\lambda}{4\pi} \quad \text{------------------(6)}$$

λ is the wavelength.

The values of extinction coefficient are directly related to the absorption of light. It can be noticed that there is a slight increase of extinction coefficient values at higher energies. After that, there is an increase with increasing photon energy and this is a general behavior, this is due to scattering resulting from surface roughness.

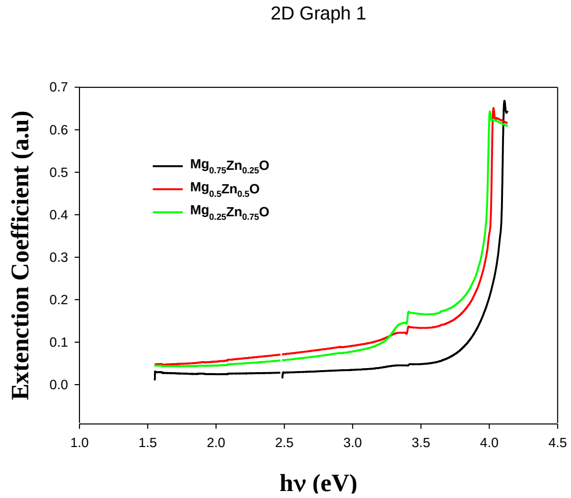


**Fig. 11:** Shows the extinction coefficient (K) of $Mg_xZn_{1-x}O$ thin films, a function of $Mg^{2+}$ composition X=(0.25, 0.5, 0.75)

## 4. Conclusions

$Mg_xZn_{1-x}O$ thin films had been deposited by spray pyrolysis method at 450°C of glass substrates. The XRD studies show that the hexagonal and cubic with a preferred grain orientation in the (002) direction, and there is a slightly shifted to larger 2θ angle with increasing x from x=(0.25 to 0.75). The $Mg^{2+}$ content greatly influences the surface morphology of $Mg_xZn_{1-x}O$ films, and an increase in $Mg^{2+}$ content increasing the grain size and surface roughness. The optical studies show that the absorption edge was found to shift toward lower wavelength (blue shift) with an increase in $Mg^{2+}$ value. The transmission values increase with the increase of $Mg^{2+}$ concentration. The band gap was increased with the increasing of $Mg^{2+}$ concentration percentage (0.25, 0.5 and 0.75). While The reflectance shifted towards the lower wavelength (high energies) with increasing $Mg^{2+}$ content. The extinction coefficient of $Mg_xZn_{1-x}O$ films have increasing values at higher energies.

## 5. Acknowledgments

The researchers would like to acknowledge the assistance offered by the Department of Physics in Faculty of Science ,University of Kufa/Iraq.

## 6. Reference

**[1]** H. E. Brown, "The Exciton Spectrum of Zinc Oxide,"Journal of Physics and Chemistry of Solids", Vol. 15, No. 1-2, pp. 86-89, 1960.

**[2]** T. Makino, Y. Segawa, M. Kawasaki, A. Ohtomo, R. Shiroki, K. tamura, T. yasuda and H. Koinuma, "Band gap engineering based on MgxZn1-xO and CdyZn1−yO ternary alloy films", Appl. Phys. Lett., Vol. 78, p1237, 2001.

**[3]** T. Makino, C. H. Chia, N. T. Tuan, Y. Segawa, M. Kawasaki, A. Ohtomo, K. Tamura, and H. Koinuma, "Room-temperature luminescence of excitons in ZnO/(Mg,Zn)O multiple quantum wells on lattice-matched substrates", Appl. Phys. Lett. Vo1. 77, p. 1632, 2000.

**[4]** T. Gruber, Kirchner, R. Kling, F. Reuss, and A. Waag F. Bertram, D. Forster, and J. Christen M. Schreck, "Optical and structural analysis of ZnCdO layers grown by metalorganic vapor-phase epitaxy", Appl. Phys. Lett. Vol. 83, p. 3290, 2003.

**[5]** M. Lorenz, E. M. Kaidashev, A. Rahm, Th. Nobis, J. Lenzner, G. Wagner, D. Spemann, H. Hochmuth, and M. Grundmann, "MgxZn1-xO (0⩽x<0.2) MgxZn1-xO (0⩽x<0.2) nanowire arrays on sapphire grown by high-pressure pulsed-laser deposition", Appl. Phys. Lett. Vol. 86, p. 143113, 2005.

**[6]** W. Yang, S.S. Hullavarad, B. Nagaraj, I. Takeuchi, R.P. Sharma, T. Venkatesan, " MgxZn1-xO on Si (100) for deep ultraviolet photodetectors", Appl. Phys. Lett. Vol. 82 p.3424, 2003.

**[7]** A.K. Sharma, J. Narayan, J.F. Muth, C.W. Teng, C. Jin, A. Kvit, R.M. Kolbas, O.W. Holland, "Optical and structural properties of epitaxial MgxZn1-xO alloys", Appl. Phys. Lett.,Vol. 75 p. 3327, 1999.

**[8]** Z. Vashaei, T. Minegishi, H. Suzuki, T. Hanada, M. W. Cho,b) and T. Yao,"Structural variation of cubic and hexagonal MgxZn1−xO layers grown on MgO,,111 c-sapphire" Journal of Applied Physics, Vol. 98, pp.054911, 2005.

**[9]** H. Chen, J. Ding, S. Ma, "Structural and optical properties of ZnO: Mg thin films grown under different oxygen partial pressures", Physica, Vol. 42, pp. 1487– 1491, 2010.

**[10]** C. Tian, D. Jiang, Z. Tan, Q. Duan, R. Liu, L. Sun, J. Qin, J. Hou, S. Gao, Q. Liang, J. Zhao, "Effects of thermal treatment on the MgxZn1_xO films and fabrication of visible-blind and solar-blind ultraviolet photodetectors", Mater. Res. Bull. Vol. 60, pp. 46–50, 2014.

**[11]** M.H. Huang, Y. Wu, H. Feick, N. Tran, E. Weber, P. Yang, "Catalytic growth of zinc oxide nanowires by vapour transport", Adv. Mater. Vol. 13, p. 113, 2001.

**[12]** S.S. Hullavarad, N.V. Hullavarad, D.E. Pugel, S. Dhar, T. Venkatesan, R.D. Vispute, "Structural and chemical analysis of pulsed laser deposited MgxZn1-xO hexagonal (x=0.15, 0.28) and cubic (x = 0.85) thin films", Opt. Mater. Vol. 30, pp. 993–1000, 2008.

**[13]** V.P. Ahirwar, P. Misra, G. Ahirwar, "A study on structural and optical properties of MgxZn1-xO thin films using pulsed laser deposition (PLD)", Res. J. Phys. Sci. Vol. 1, pp. 11–14, 2013.

**[14]** M. Chaari, A. Matoussi and Z. Fakhfakh, "Structural and Dielectric Properties of Sintering Zinc Oxide Bulk Cer- amic," Materials Sciences and Application, Vol. 2, No. 7, pp. 764-769, 2011.

**[15]** Zayani Jaafar Othman and Adel Matoussi, "Structural and Optical Properties of Znx−1MgxO Ceramic Composites", Journal of Materials Sciences and Applications, , Vol. 3, pp. 538-542, 2012.

**[16]** L.E. Smart and E.A. Moore, "Solid State Chemistry", Taylor & Francis Group Boca Raton London New York Singapore, 2005.

**[17]** S. Rajathi, N. Sankarasubramanian, K. Ramanathan, M. Senthamizhselvi, "Structural and Optoelectronic Properties af Pyralytically Sprayed CdZnS Thin Films", Chalcogenide Letters, Vol. 9, PP. 495–500, 2012.

**[18]** Naoki Nishimoto and Katsumi Yoshino, "Evaluation of ZnO-MgO Mixed Thin Films Grown by Metal-Organic Decomposition", e-J. Surf. Sci. Nanotech. Vol. 13, pp. 185-189, 2015.

**[19]** L. S. Ravangave, and U. V. Biradar, "Study of Structural, Morphological and Electrical Properties of CdxZn1-xS Thin Films", IOSR J. of Applied Physics, Vol. 3, PP. 41-47, 2013.

**[20]** Sze, S.M. and Kwok, K.,Ng., "Physics of Semiconductor Devices", Third Edition, John Wiley & Sons, Jnc. Publication, 2007.

**[21]** S. Han, J.Y. Zhang, Z.Z. Zhang, Y.M. Zhao, D.Y. Jiang, Z.G. Ju, D.Z. Shen, D.X. Zhao, B. Yao, "The substrate effect on the optical band gap of the Mg0.53Zn0.47O thin films", Materials Chemistry and Physics, Vol. 125, pp. 895–898, 2011.

**[22]** A. Ohtomo, M. Kawasaki, T. Koida, K. Masubuchi, H. Koinuma, Y. Sakurai, Y. Yoshida, T. Yasuda, Y. Segawa, "MgxZn1−xO as a II-VI Widegap Semiconductor Alloy", Applied Physics Letters, Vol. 72, No.19, pp. 2466-2468, 1998.

**[23]** Mindaugas Karali unas, Vilmantas Sukauskas, Edmundas Kuokstis, Shao-Ying Ting, Jeng-Jie Huang, and C.-C. Yang, "Band tail filling effect in MBE grown ternary MgZnO epitaxial layers with high Mg content", Phys. Status Solidi, No. 10, PP. 1265-1267, 2012.

**[24]** L.K. Wanga, b, Z.G. Jua, b, C.X. Shana, J. Zhenga, b, B.H. Lia, Z.Z.

Zhanga, B. Yaoa, D.X. Zhaoa, D.Z. Shena, J.Y. Zhanga, "Epitaxial growth of high quality cubic MgZnO films on MgO substrate", Journal of Crystal Growth, Vol. 312, pp. 875–877.

**[25]** V. Ganesh, I.S. Yahia, S. Alfaify, Mohd. Shkir, "Sn-doped ZnO nanocrystalline thin films with enhanced linear and nonlinear optical properties for optoelectronic applications", Journal of Pysics and Chemistry of Solids, vol. 100, pp. 115–125, 2017.

**[26]** Adel H. Omran Alkhayatt, and Shymaa K. Hussian,"Fluorine Dopant Concentration Effect on the Structural and optical Properties of Spray Deposited Nanocrystalline ZnO Thin Films" Surface and Interfaces, Vol. 8, PP. 176-181, 2017.